



ELSEVIER

Available online at www.sciencedirect.com

Journal of Magnetism and Magnetic Materials 311 (2007) 238–243

www.elsevier.com/locate/jmmm

Magnetic movement of biological fluid droplets

Antonio A. García^{a,*}, Ana Egatz-Gómez^a, Solitaire A. Lindsay^a, P. Domínguez-García^c, Sonia Melle^{a,b}, Manuel Marquez^{a,g}, Miguel A. Rubio^c, S.T. Picraux^{d,h}, Dongqing Yang^d, P. Aella^d, Mark A. Hayes^e, Devens Gust^e, Suchera Loyprasert^f, Terannie Vazquez-Alvarez^f, Joseph Wang^f

^aHarrington Department of Bioengineering, Arizona State University, Tempe, AZ 85287, USA

^bDepartamento de Óptica, Universidad Complutense de Madrid, Arcos de Jalón s/n, Madrid 28037, Spain

^cDepartamento de Física Fundamental, UNED, Senda del Rey 9, Madrid 28040, Spain

^dDepartment of Chemical and Materials Engineering, Arizona State University, Tempe, AZ 85287, USA

^eDepartment of Chemistry and Biochemistry, Arizona State University, Tempe, AZ 8528, USA

^fBiodesign Institute, Arizona State University, Tempe, AZ 85287, USA

^gResearch Center, Philip Morris USA, Richmond, VA 23234, USA

^hLos Alamos National Laboratory, MST-CINT, Los Alamos, NM 87545, USA

Available online 14 December 2006

Abstract

Magnetic fields can be used to control the movement of aqueous drops on non-patterned, silicon nanowire superhydrophobic surfaces. Drops of aqueous and biological fluids are controlled by introducing magnetizable carbonyl iron microparticles into the liquid. Key elements of operations such as movement, coalescence, and splitting of water and biological fluid drops, as well as electrochemical measurement of an analyte are demonstrated. Superhydrophobic surfaces were prepared using vapor–liquid–solid (VLS) growth systems followed by coating with a perfluorinated hydrocarbon molecule. Drops were made from aqueous and biological fluid suspensions with magnetizable microparticle concentrations ranging from 0.1 to 10 wt%.

© 2006 Elsevier B.V. All rights reserved.

Keywords: Drop; Microfluidics; Paramagnetic particle; Superhydrophobic surface; Carbonyl iron microparticle; Nanowire; Albumin; Serum

1. Introduction

Early detection can have a profound impact on treatment outcomes and mitigation of damage for a variety of illnesses including cancer, cardiovascular disease, Alzheimer's and Parkinson's diseases. One of the barriers to early detection is a platform needed to run tests in a timely fashion. Molecular diagnostic technologies are an important facet of rapid testing. Encompassing the complete range of molecular diagnostics are the user friendly and simpler, rapid, point-of-care technologies for specific disease markers and, on the other end of the spectrum, sophisticated strategies to detect the presence and concentration of a wide range of molecules using the

so-called “omic” analyses (e.g. genomic, proteomic). Both approaches can benefit from tools that can manipulate small amounts of biological fluid samples, separate components within these samples, and run a series of analyses that create a “profile” of the sample being tested.

Towards the goal of developing equipment platforms that work with small amounts of biological fluid samples, our research laboratories have been studying how to control the properties of a surface so that biological fluids can be handled without the use of a container. In recent years, many researchers have concentrated their attention on actuation of liquid contact angle changes by chemical modification of the surface [1,2] or by using external stimuli, such as light [3] or electric fields [4]. A major goal in this area has been to control phenomena related to wetting, such as capillary rise and fall and the movement of liquid drops along surfaces using gradients. For instance,

*Corresponding author. Tel.: +1 480 965 8798.

E-mail address: tony.garcia@asu.edu (A.A. García).

wettability gradients induced by a chemical reaction at the substrate underneath the drop have been reported [5–7]. Thermal gradients controlled by a laser beam have also been used to move droplets at low speeds [8], while asymmetric lateral vibration induced a net inertial force that displaces drops [9]. There have been studies on the dynamics of drops rolling over an inclined superhydrophobic surface through the action of gravity [10,11]. Also, the movement of emulsion droplets stabilized by carbonyl iron microparticles in an oil–water system were recently investigated [12]. Although drop dynamic behavior on a superhydrophobic surface is interesting from a scientific and technological point of view, little is known about aqueous drops moving on a level, non-patterned superhydrophobic surface by mechanisms different from gravity. Several technologies can benefit from key advances in this field, such as superhydrophobic surfaces capable of self-cleaning by the action of a rolling drop [13,14] or microfluidic devices that take advantage of new effects and of better performance derived from manipulating fluids at small scales [15]. In contrast to these efforts, our approach has been to control aqueous drops rather than simply having them be repelled by the surface. Droplet or “Digital” microfluidics is an alternative paradigm to channel-based techniques where fluid is processed in unit-sized packets, which are transported, stored, mixed, reacted, or analyzed in a discrete manner [16]. This concept has already been demonstrated using electrowetting arrays for droplet transportation without the use of pumps or valves [16–18]. In our case, we have developed a method for moving drops of biological fluids using magnetic fields. A notable difference in our overall approach is that we are using an open drop format (using a sample holder with controlled humidity) so that an array of detection systems can be used and drop movement can be conducted very rapidly due to low frictional and viscous resistance to flow. Control over humidity can also allow us to concentrate the drop after a dilution or drop-combining step.

In this paper, we report on a novel method to displace, coalesce and split carbonyl iron microparticle-containing drops of water or biological fluids on flat, nonpatterned, silicon nanowire, superhydrophobic surfaces with the only driving force being the use of magnetic fields. Because of the similarity it bears with digital microfluidics by electrowetting, we have named this phenomena digital magnetofluidics.

2. Experimental methods

Superhydrophobic surfaces were prepared using a vapor–liquid–solid (VLS) growth process to create high aspect ratio silicon nanowires [19]. Briefly, gold nanodots are formed by vapor deposition onto a Si surface and used to catalyze the growth of Si nanowires in a low pressure chemical vapor deposition system. In these experiments, the surfaces contained nanowires exhibiting multi-dimensional, random roughness with diameters ranging from 20

to 50 nm and with a height of approximately 2 μm . The separation distance between nanowires was from 60 to 100 nm. The nanowire substrates were rendered hydrophobic by covalently applying a perfluorinated hydrocarbon (1H,1H, 2H, 2H-perfluorooctyltrichlorosilane) coating to the entire surface. This combination of nanoscale topography and hydrophobic coating resulted in surfaces where drop contact angles approached 180°.

We used carbonyl iron particles (Sigma-Aldrich Inc., St Louis, MO) with sizes ranging from 6 to 9 μm . These microparticles exhibit high magnetic saturation and are commonly used in experimental studies and technological applications on magneto-rheological fluids [20]. In simple terms, when an external magnetic field H is applied, a net magnetic dipole moment aligned with the external field is induced in the particles. This magnetic moment is $m = (4\pi/3) a^3 M$, with $M = \chi H$, where M is the magnetization of the particle, a is its radius, and χ is the magnetic susceptibility. Therefore, the induced magnetic dipoles of the microparticles align with the external magnetic field lines, causing the formation of clusters. These particles are usually regarded as paramagnetic or superparamagnetic, because their magnetization curve (M – H curve) has a small or null hysteresis, little or no magnetic remanence, and their magnetic response is linear for applied magnetic fields of small intensity [12].

For this study, carbonyl iron microparticles were coated with polysiloxane following the procedure described by Pu et al. [21] to prevent oxidation. Iron–polysiloxane composites were prepared by hydrolysis–condensation polymerization of tetraethylorthosilicate (Sigma-Aldrich Inc., St. Louis, MO). Iron particles (20 g) were added to a mixture of tetraorthosilicate (40 ml) and ethyl alcohol (160 ml) and stirred. Next, 10 ml of ammonium hydroxide (25 wt%; Sigma-Aldrich Inc., St. Louis, MO) was slowly added to the mixture, which was then stirred for 24 h at room temperature. Coated particles were washed three times with ethyl alcohol, four times with deionised water, and dried at 60 °C in a vacuum oven for 24 h. Fig. 1(a) shows a SEM image of polysiloxane-coated carbonyl iron microparticles. Based on this and other images, the particle coating was estimated to be 60 nm in thickness. Fig. 1(b) shows the field dependent magnetization of the samples, characterized at 300 K using a quantum design vibrating sample magnetometer (VSM). This magnetometer was equipped for the physical property measurement system (PPMS) with an applied magnetic field of 10 kOe in order to reach saturation values. Both uncoated and the coated microparticles exhibited negligible hysteresis as described by others using iron carbonyl particles [21]. Notably, the polysiloxane coating only slightly affected the magnetic properties of the particles, reducing the magnetic saturation value of the carbonyl iron microparticles from approximately 225 to 191 emu/g and increasing the coercive force from approximately 1.3 Oe for the uncoated microparticles to 6.5 Oe for the polysiloxane-coated microparticles. The change in microparticle magnetic properties,

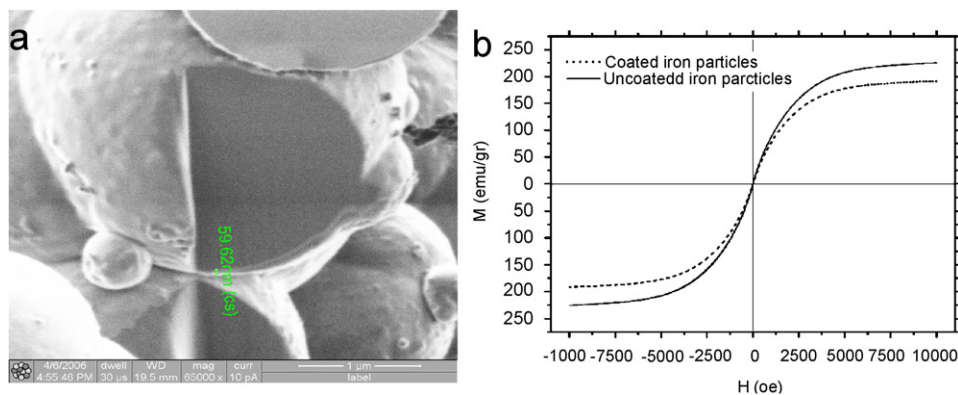


Fig. 1. (a) SEM image showing the polysiloxane-coated carbonyl iron microparticles. (b) Magnetization curve for both uncoated and polysiloxane-coated carbonyl iron microparticles.



Fig. 2. Still frames from a video showing the movement of a 20 μ l water drop containing 2% carbonyl iron particles. The drop moves from left to right by the action of a permanent magnet that is manually displaced below the surface and reaches a maximum speed of about 2 cm/s.

also, did not visibly affect the magnetically-controlled drop movement observed in this study.

Drops (20 μ l) from several biological fluids, containing 2% polysiloxane-coated iron particles were pipetted onto the superhydrophobic silicon nanowire surface and observed. These fluids included deionised water supplemented with 8% bovine serum albumin (BSA; Rockland Immunochemicals Inc., Gilbertsville, PA), fetal bovine serum (VWR, West Chester, PA), and whole bovine blood supplemented with the anti-coagulant, K_3 EDTA (Innovative Research Inc., Southfield, MI). A NdFeB cylindrical (6.44 mm diameter and 12.7 mm length) rare earth magnet (Magcraft, NSN0718/N40) with residual flux density (Br) of 12800 Gauss, coercive force (H_{cb}) of 11900 Oe, and maximum energy product (BHmax) of 40 MGOe, was positioned directly below the superhydrophobic surface and moved by hand. The directed movement of these drops was recorded using an Optura 20 Canon digital camcorder (Canon, Lake Success, NY). Snapshots from the videos were analyzed to obtain an approximate value of the maximum drop velocity. Static and dynamic contact angles were determined using the contact angle tool in Image J (National Institutes of Health, <http://rsb.info.nih.gov/ij>).

3. Results and discussion

Initial studies were conducted with deionised water. Drops containing a suspension of coated carbonyl iron microparticles were added to the superhydrophobic surface and directed to move by a NdFeB magnet. In this study, drop movement was studied as a function of size and

particle concentration. Drops followed the magnet motion with particle concentrations as small as 0.1% in weight, and along a 2 cm linear path at speeds up to 7 cm/s, and in a circular path. Fig. 2 shows still images from a typical video, where a paper grid with boxes of a tenth of an inch in width is given as a reference. Water drops moved effortlessly and responded quickly to magnet displacement. After observing this phenomenon, one could argue that the drop is sliding across the surface. However, it could also be argued that the particles are moving over the surface of the water drop in a “tank-treading” like motion, or in a better analogy, as a pet hamster would move when placed inside of a plastic play ball. When a small piece of Styrofoam is placed on top of a water drop, the Styrofoam remains virtually motionless as the drop moves across the superhydrophobic nanowire surface. Thus we conclude that the water drop slides along the surface due to the combined effects of a superhydrophobic surface and the very low amount of contact area between the rounded water drop and the nanowire surface. A first order analysis of this type of drop motion is derived below.

When the magnet is displaced, the clusters follow the magnet motion, sliding inside the drop, until they arrive at the contact line. When the more advanced cluster arrives at the contact line, the competition between capillary force and magnetic force causes the cluster to start climbing along the drop surface as depicted in Fig. 3. The magnetic force acts along the cluster axis, while the capillary force acts along the normal to the drop surface. The vertical component of the magnetic force will then deform the drop surface at the contact line towards the superhydrophobic

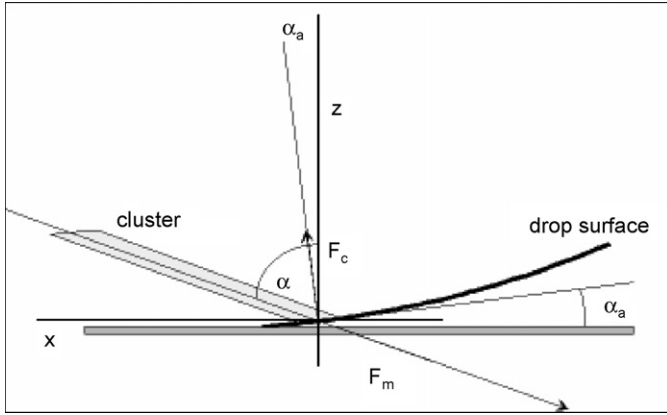


Fig. 3. A schematic force diagram illustrating that the vertical component of the magnetic force F_m deforms the drop surface at the contact line towards the superhydrophobic surface. This results in an increase in the advancing contact angle based on the relationship $\theta_a = \pi - \alpha_a$.

surface. Hence, α_a ($\alpha_a = \pi - \theta_a$) decreases and the advancing contact angle, θ_a , increases. Consequently, the magnetic force builds a difference between the contact angles at the advancing and the receding parts of the contact line. This contact angle difference opposes the drop motion with a force that can be expressed as $2\gamma rJ$ [22], where γ is the surface tension, $r = R \cos(\theta_c - \pi/2)$ is the radius of the circle of contact between the drop and the superhydrophobic surface with R being the radius of the drop, and $J = \cos \theta_a - \cos \theta_r$ where θ_r is the receding contact angle. At equilibrium, the total horizontal force balance on the drop can be written as follows:

$$F^m \sin \alpha - \frac{\pi\gamma D}{\cos(\alpha - \alpha_a)} \sin \alpha_a - 2\gamma R \cos\left(\theta_c - \frac{\pi}{2}\right) \times (\cos \theta_a - \cos \theta_r) = 0,$$

where F^m is the modulus of the magnetic force on the cluster, α is the angle that the magnetic force forms with the vertical axis, and D is the diameter of the cluster. For completeness, the vertical force balance reads:

$$F^m \cos \alpha - \frac{\pi\gamma D}{\cos(\alpha - \alpha_a)} \cos \alpha_a = 0.$$

If there is no difference between the advancing and receding contact angles, the force balance equations simply state that the system would be in equilibrium provided $\alpha = \alpha_a$. Instead, when a contact angle difference is produced, the capillary force that opposes the contact line motion introduces a threshold that can only be overcome when the inclination of the clusters, α , is larger than the advancing contact angle, α_a . This is precisely what would happen in the situation depicted in Fig. 3, where the vertical components of magnetic and capillary force compensate, while the magnetic force horizontal component is visibly higher than the corresponding capillary component. When this excess magnetic force horizontal component is higher than the contact angle difference term, drop motion will occur. From this point of view, large

values of α would be more convenient in order to overcome the opposing force due to the contact angle difference.

It may be possible that the first cluster arriving at the contact line would not be able to overcome the capillary retention force. Then the magnet displacement with respect to the drop will keep increasing, making the first cluster climb along the drop surface and driving more clusters to the contact line. Due to the magnetic field spatial structure, the clusters arriving at the contact line would have a larger inclination, which will then create a comparatively stronger contribution to the horizontal component of the magnetic force than the vertical component. Consequently, the advancing contact angle would be slightly perturbed, while the horizontal force will increase significantly and drop motion will occur. This is precisely what happens in our experiments, as shown in Fig. 2, where the contact angle difference and the inclination of the clusters can be appreciated.

A full numerical check of the above expressions is not possible, however, because precise values concerning the size and the number of the clusters would be needed. This possibility is precluded by the lens effect of the drop surface. Nevertheless, calculations based on the actual measured values of the angular variables of the problem ($\theta_c \approx 147^\circ$, $\theta_a \approx 160^\circ$, $\theta_r \approx 136^\circ$, and $\alpha \approx 44^\circ$) show that the order of magnitude of the magnetic force modulus needed to balance the capillary and retention forces is within the range achievable in our experimental setup.

Another interesting aspect is the role of the magnet velocity in the initiation of drop motion. Actually, the magnet displacement entrains the cluster structure in its motion. Before the threshold condition for drop motion is achieved, the drop is standing and the clusters move through it with possibly large velocities. In order to make some estimations, the clusters appearing in the experiments can be approximated as circular cylinders of, say, diameter $D = 100 \mu\text{m}$. These clusters may move within the standing drop at speeds V up to 10 cm/s. These values ($D = 100 \mu\text{m}$, $V = 0.1 \text{ m/s}$, and using the density and the viscosity of water) yield a Reynolds number: $\text{Re} = \rho V D / \mu \approx 10$. This means that inertial effects of the fluid may be important at these high magnet speeds.

Finally, the sliding motion of the drops deserves some comments. Fluid drops surrounded by another fluid can show multiple types of motion depending on drop shape, drop size, and viscosity contrast. For instance, slipping, sliding, rolling, and tank-treading motions have been described [23] in the case of drops slowly moving under gravity body force on inclined plates. In such a case, the shape of the drop is controlled by the Bond number, $\text{Bo} = \Delta\rho g R^2 / \gamma$, where $\Delta\rho$ is the density difference between both fluids, g is the acceleration due to gravity, and R is the radius of the drop. Low Bo values correspond to drops with virtually undeformed spherical shape, medium Bo values correspond to drops considerably flattened in contact with the plate, and high Bo values correspond to pancake shaped drops. It is known [23] that flattened and

pancake drops with higher viscosities than the surrounding fluid should exhibit a sliding motion. In the experiments reported here, we are dealing with flattened water drops in air (e.g. a high viscosity contrast condition). Therefore, sliding motion should be expected. Nevertheless, a caveat is in order here. Namely, the above mentioned analysis [23] pertains to Stokes flow induced by a gravity body force and with buoyancy as the drop deforming force. However, in our experiments motion is caused by forces applied to the drop surface; the deformation of the drop is due to this same surface force, not to flow.

Drop motion experiments with an aqueous solution of BSA and serum were also conducted. Both of these biological fluids were moved, though differences in contact angles and in motion were observed. Table 1 shows that while the static advancing angle is very similar for water, BSA solution, and serum, the dynamic angles are very different. Before we conducted these experiments, we studied the behavior of these solutions as well as saliva, urine, plasma, and whole blood on superhydrophobic surfaces without magnetic particles. Our overall conclusion from those experiments is that viscous biological fluid drops have a high contact angle on superhydrophobic surfaces, but sometimes do not roll off the surface. Our preliminary hypothesis to explain this behavior is that viscoelastic fluids create a higher amount of friction than

water presumably due to their ability to deform around the tops of the nanowires. When we move drops of BSA solution or serum using magnetic particles under the influence of a magnetic field, they appear to move more sluggishly than water.

Coalescence and/or splitting of drops are also steps with practical utility in microfluidics. We have achieved coalescence of two drops as seen in Fig. 4 by moving two particle-laden BSA-containing drops towards each other using two magnets. The resulting coalesced drop can also be moved with the magnet. Drop splitting can also be achieved for a drop with a higher concentration of paramagnetic particles (5%), by means of two magnets that are placed below the superhydrophobic surface. As seen in Fig. 5, by placing two magnets with poles oriented in the same direction under one BSA containing drop and progressively separating the two magnets, the drop was deformed until it split. In this Fig., the resultant drops are unequal in size. Interestingly, when water drops are split the resultant drops appear nearly identical in size. In general, we have observed that it is more difficult to create two drops of equal sizes in BSA solution than with water, possibly due to the viscoelastic properties of the BSA solution.

After establishing the ability to move, coalesce, and split drops, we have conducted some simple experiments to show that we can use electrochemical techniques to analyze the contents of a drop. Fig. 6 shows a sequence of still images from a video where a drop is moved to a microelectrode system for dopamine analysis in aqueous solution. Measurements can be taken to determine the dopamine concentration of a drop. We have initiated experiments to automate the system to include wash and rinse steps in order to rapidly and accurately measure the concentration in more than one drop. At this juncture, we have observed that the drop coating protects the iron particles from any unwanted reactions that would cause a false reading or create impurities within the drop. It is

Table 1
Comparison of contact angles for water and biological solutions for drops controlled on a superhydrophobic surface using paramagnetic particles and an external magnetic field

Fluid	Average static advancing angle	Average dynamic advancing angle	Average dynamic receding angle
Distilled water	142	149	137
BSA solution	146	112	101
Serum	137	92	83

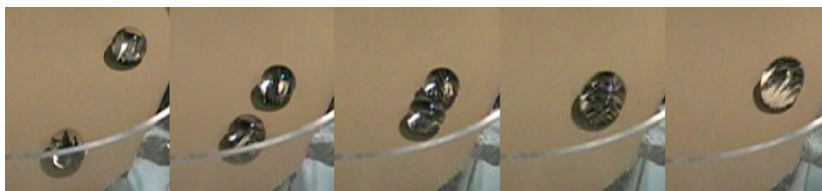


Fig. 4. A sequence of still frames from a video showing coalescence of two albumin solution drops.

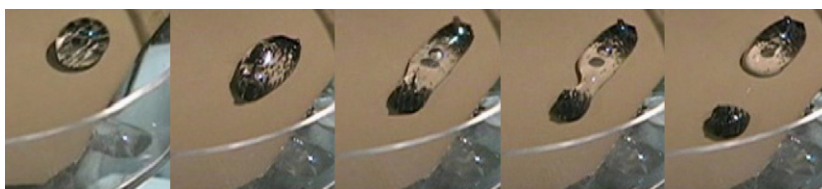


Fig. 5. A sequence of still frames from a video where an albumin drop is split by the action of two bar magnets being separated underneath the superhydrophobic surface.

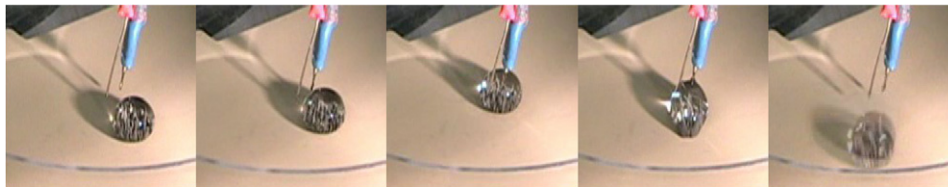


Fig. 6. A sequence of still frames from a video showing a dopamine aqueous solution drop being moved towards an electrode by the action of a magnet, and pulled away from the electrode after the measurement is completed.

fortuitous that the use of a magnetic field to move the drop also serves to pin the drop on the surface, thus preventing capillary action from wicking the drop up the microelectrode assembly.

4. Conclusions

The combination of a superhydrophobic surface and paramagnetic particles controlled by a magnetic field can be used to move, coalesce, and split drops of water and biological fluids. Visual observations of water drop movement indicate that drops slide along the superhydrophobic nanowire surface. Drop movement is due to the formation of particle chains under the influence of a magnetic field, which press against the surface of the drop and overcome capillary and surface friction forces. Because biological fluids contain biopolymers that make the solution viscoelastic, dynamic contact angles are lower for these solutions and hence, they move more sluggishly. Employing two independent magnetic fields allows for useful drop manipulation such as coalescence and splitting. This system of drop control is also amenable to analytical techniques such as electrochemistry, and suggests that digital magnetofluidics is a promising new method for rapid detection and analysis in diagnostic applications.

Acknowledgments

This work was supported in part by the Interdisciplinary Network of Emerging Science and Technologies (INEST) and More Graduate Education at Mountain States Alliance (MGE@MSA). In addition, financial support (for D.Y., P.A. and S.T.P.) by the National Science Foundation (DMR-0413523) is gratefully acknowledged.

References

- [1] A. Otten, S. Herminghaus, *Langmuir* 20 (2004) 2405.
- [2] C. Journet, S. Moulinet, C. Ybert, et al., *Europhys. Lett.* 71 (2005) 104.
- [3] R. Rosario, D. Gust, A.A. Garcia, et al., *J. Phys. Chem. B* 108 (2004) 12640.
- [4] S.A. Morton, D.J. Keffer, R.M. Counce, et al., *Langmuir* 21 (2005) 1758.
- [5] F. Domingues Dos Santos, T. Ondarcuchu, *Phys. Rev. Lett.* 75 (1995) 2972.
- [6] S.W. Lee, D.Y. Kwok, P.E. Laibinis, *Phys. Rev. E* 65 (2002) Art No. 051602.
- [7] U. Thiele, K. John, M. Bar, *Phys. Rev. Lett.* 93 (2004) 27802.
- [8] K.T. Kotz, K.A. Noble, G.W. Faris, *Appl. Phys. Lett.* 85 (2004) 2658.
- [9] S. Daniel, M.K. Chaudhury, P.G. de Gennes, *Langmuir* 21 (2005) 4240.
- [10] D. Quéré, D. Richard, *Europhys. Lett.* 48 (1999) 286.
- [11] L. Mahadevan, Y. Pomeau, *Phys. of Fluids* 11 (1999) 2449.
- [12] S. Melle, M. Lask, G.G. Fuller, *Langmuir* 21 (2005) 2158.
- [13] D. Quéré, *Nat. Mat.* 1 (2002) 14.
- [14] P. Gould, *Mat. Today* 6 (2003) 44.
- [15] N.T. Nguyen, S.T. Wereley, *Fundamentals and Applications of Microfluidics*, Artech House, Norwood, MA, 2002.
- [16] R. Fair, *Digital Microfluidics* (2004) cited 2005 11/01. Available from <<http://www.ee.duke.edu/research/microfluidics/>>.
- [17] V. Srinivasan, V.K. Pamula, R.B. Fair, *Anal. Chim. Acta* 507 (2004) 145.
- [18] H. Ren, et al., *Sens. Act. B: Chem.* 87 (2002) 201.
- [19] J.W. Dailey, J. Taraci, T. Clement, et al., *J. Appl. Phys.* 96 (2004) 7556.
- [20] R.I. Vardarajan, 1947. US patent 2,417,590; J.M. Ginder, L.D. Elie, L.C. Davis, US patent 5,549,837.
- [21] H. Pu, F. Jiang, Z. Yang, *Mat. Lett.* 60 (2005) 94.
- [22] C.G.L. Furmidge, *J. Colloid Sci.* 17 (1962) 309.
- [23] S.R. Hodges, O.E. Jensen, J.M. Rallison, *J. Fluid Mech.* 512 (2004) 95.